MODELING AND SIMULATION OF A WET HEMIHYDRATE PHOSPHORIC ACID PROCESS

Hyun Jun Cho, Yeong-Koo Yeo[†], Woo Hyun Park* and Bong Kyu Moon*

Dept. of Chem. Eng., Hanyang University, Seoul 133-791, Korea
*Namhae Chemical Co., Nakpodong, Yeochun 555-250, Korea

Abstract – The wet hemihydrate phosphoric acid process was modeled and simulated with some assumptions and simplifications. The process consisted of grinding unit, reaction section, filtration section, and hydration unit and steady-state operation was assumed. Modeling was based on actual operation data and models for each unit were combined to form the overall closed system. Results of simulations showed that the model developed in this study described the behavior of actual plant very well. Various sensitivity analyses for the fundamental parameters were performed using the model. In grinding section, the effect of specific breakage rate on particle size distribution was examined. It was possible to regulate the temperature of slurry at reaction and hydration stage by using slurry recycle ratio. The effects of the recycle ratio on phosphoric acid concentration were also investigated.

Key words: Hemihydrate, Phosphoric Acid, Modeling, Simulation

INTRODUCTION

There are two general methods used for the manufacture of phosphoric acid. In the first, known as the wet process, phosphate rock is treated with a sufficient amount of sulfuric acid to convert completely the P_2O_5 content into orthophosphoric acid. The second is the furnace method in which phosphate rock is fused in the presence of reducing materials. Elemental phosphorus is produced and burned with air to form P_2O_5. This is absorbed in water to give an acid of high uniform purity. In general, and under prevailing economic conditions, it is substantially cheaper to make phosphoric acid by the wet process than by the thermal reducing process. Therefore the wet process accounts for more than 90% of the current phosphoric acid production.

Wet phosphoric acid process essentially consists of attack of sulfuric acid on phosphate rock and separation of the product acid from the resulting calcium sulfate crystals. The type of crystals which are generated from reaction depends on temperature and P_2O_5 concentration in reacting slurry. Hemihydrate crystal ($CaSO_4 \cdot 1/2H_2O$) is formed at relatively high temperature and high P_2O_5 concentration. In the HDH (hemidihydrate) process hemihydrate crystallization occurs followed by recrystallization to dihydrate which has good filterability [Becker, 1989]. In spite of some difficulties in operation and high equipment cost, HDH process is getting more popular due to many advantages such as the production of strong acid and pure gypsum, less consumption of sulfuric acid and high efficiency, etc.

In this work modeling and simulation of actual hemihydrate plant, especially of HDH process, for the production of phosphoric acid were performed. A few researchers [Becker, 1987; Clayton et al., 1984; Yeo et al., 1991] presented some works

on dihydrate process which was widely used in the past. On the other hand, there have been little studies on hemihydrate process. Giola et al. [1977] presented some simulation results for hemihydrate process but the system which was modeled is so simple that it may not be applied to real plant. In the present study the phosphoric acid plant at Namhae Chemical Co. was modeled and operational behavior was investigated in detail. But the real plant is too complex and few operational data were available. So the model was simplified within the range of not losing its characteristics and some assumptions were made for the system. From simulations, it was found that a reasonable description of the process was possible and the analysis of the effects of some fundamental operating parameters was performed to identify optimal operating conditions.

DESCRIPTION OF THE OVERALL PROCESS

The HDH process is a new technology for the production of phosphoric acid in that recrystallization unit is added to the conventional dihydrate process. The main objectives in the operation of the phosphoric acid plant are:

(1) to extract the maximum amount of P_2O_5 from the phosphate rock fed to the plant;

(2) to generate crystals which are easily filterable;

and (3) to produce phosphoric acid with as high P_2O_5 concentration as possible.

The HDH process is composed of phosphate rock grinding unit, reaction unit, hemihydrate filtration unit, hydration unit and dihydrate filtration unit. Fig. 1 shows a simplified structure of a typical HDH process. Each unit in the HDH process can be classified into 3 sections, that is, grinding section, hemihydrate section and dihydrate section. In grinding section, coarse rock is broken into small-sized particles so that they have sufficiently large surface area in order to increase the reaction ef-
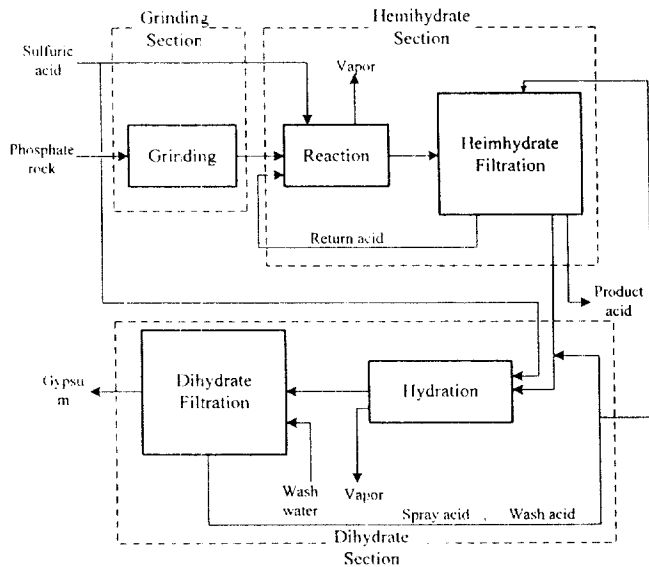

Fig. 1. A simplified structure of HDH process.

Fig. 2. Structure of grinding section.

ficiency. The ground rock particles and sulfuric acid are fed into reactors where dissolution of phosphate rock and crystallization into hemihydrate take place. The reactors are held at 90-100°C by vacuum cooling to produce slurry containing hemihydrate crystals and phosphoric acid solution. The slurry from reaction unit is filtered to give 45-50% P_2O_5 product acid and return acid and resulting hemihydrate cake is transferred to hydration tank. In hydration tank, at which the temperature is maintained approximately at 60°C by vacuum cooling, hemihydrate crystals and unreacted rock are converted into dihydrate crystals. The dihydrate crystals (gypsum) are washed in dihydrate filter and retreated with pond water for some additional treatments. In the HDH process, strong acid and pure gypsum can be obtained because the acid is produced at hemihydrate region directly, and final filter cake is obtained by two-step filtration.

GRINDING SECTION

The purpose of grinding is to make dissolution of rock more efficient by reducing the size of coarse rock, namely, by increasing the surface area of feed rock. At reaction step, relatively large particles the size of which is over 200 μm can be coated with other crystals and wouldn't be dissolved any more. Therefore, for optimal operation, it is imperative to keep the size of the particle well below 200 μm.

Grinding section consists of more than 10 relevant equipments but it can be simplified into the system which has 2 units as shown in Fig. 2. Before being introduced into the grinding section, unground rock flow is screened and divided into two parts. Undersized rock is conveyed to rock storage silo directly, but oversized rock is fed to ball mill in grinding section. At the ball mill, coarse rock is ground to fine particles which are blown off to the separator by fan. From the separator oversized rock particles are recycled to the ball mill and undersized ones are transferred to the silo.
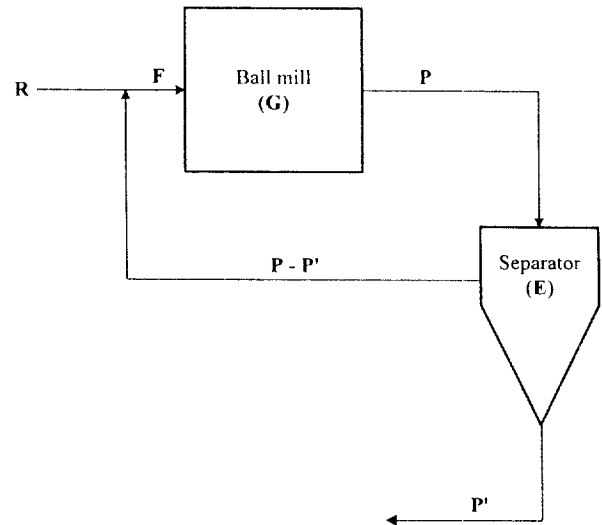
At steady-state operation, suppose that unground rock, **R**, is

introduced into grinding section and that it has size distribution given by

$$\mathbf{R}^T = [r_1 r_2 \cdots r_n] = r_t [x_{R,1} \; x_{R,2} \cdots x_{R,n}] \tag{1}$$

R is merged with recycled stream, **P − P′**, to give **F** which is fed to the ball mill.

$$\mathbf{F} = \mathbf{R} + \mathbf{P} - \mathbf{P}' \tag{2}$$

where $\mathbf{F}^T = [f_1 \; f_2 \cdots f_n] = f_t [x_{F,1} \; x_{F,2} \cdots x_{F,n}]$

$\mathbf{F}^T = [p_1 \; p_2 \cdots p_n] = p_t [x_{P,1} \; x_{P,2} \cdots x_{P,n}]$

In the ball-mill, feed **F** is ground to fine particles, **P**, and the following equation should be satisfied.

$$p_t = f_1(g_{11} + g_{21} + \cdots + g_{n1}) + f_2(g_{22} + g_{32} + \cdots + g_{n2}) + \cdots + f_n(g_{nn})$$
$$= p_1 + p_2 + \cdots + p_n \tag{3}$$

Eq. (3) can be rewritten by using vector-matrix notations as

$$\mathbf{P} = \begin{bmatrix} p_1 \\ p_2 \\ \cdot \\ \cdot \\ p_{n1} \end{bmatrix} = \begin{bmatrix} g_{11} & 0 & 0 & \cdots & 0 \\ g_{21} & g_{22} & 0 & \cdots & 0 \\ \cdot & \cdot & \cdot & \cdots & \cdot \\ \cdot & \cdot & \cdot & \cdots & \cdot \\ g_{n1} & g_{n2} & g_{n3} & \cdots & g_{nn} \end{bmatrix} \begin{bmatrix} f_1 \\ f_2 \\ \cdot \\ \cdot \\ f_n \end{bmatrix} = \mathbf{GF} \tag{4}$$

where, **G** is the transfer matrix of the ball mill.

With the introduction of the separation efficiency, **E**, we can represent undersized stream, **P′**, and **F** as following:

$$\mathbf{P}' = \mathbf{EP} \tag{5}$$

$$\mathbf{F} = \mathbf{R} + \mathbf{P} - \mathbf{P}'$$
$$= \mathbf{R} + (\mathbf{I} - \mathbf{E}) \mathbf{P} \tag{6}$$

From Eq. (4) and (6), we have

$$\mathbf{P} = (\mathbf{I} - \mathbf{G} + \mathbf{GE})^{-1} \mathbf{GR} \tag{7}$$

$$\mathbf{P}' = \mathbf{E}(\mathbf{I} - \mathbf{G} + \mathbf{GE})^{-1} \mathbf{GR} \tag{8}$$

The elements of transfer matrix, **G**, can be obtained from

SMB (Size-Mass Balance) equations for continuous ball mill unit [Rajamani et al., 1991] and is given by

$$\frac{d}{dt}[H(t)x_{P,i}(t)] = M_F(t)x_{F,i}(t) - M_P(t)x_{P,i}(t) - S_i H(t)x_{P,i}(t)$$
$$+ \sum_{j=1}^{i-1} b_{i,j}S_j H(t)x_{P,j}(t) \qquad (9)$$

At steady-state, Eq. (9) becomes

$$0 = f_i - p_i - \tau S_i p_i + \sum_{j=1}^{i-1} b_{i,j}\tau S_j p_j \qquad (10)$$

where $\tau = \dfrac{H}{M}$, $f_i = Mx_{F,i}$, $p_i = Mx_{P,i}$

After some rearrangements of Eq. (10) we have

$$\hat{p}P = \hat{f}F \qquad (11)$$

where $\hat{p} = \begin{bmatrix} 1 & 0 & 0 & \cdots & \cdot & 0 \\ \dfrac{-b_{2,1}\tau S_1}{1+\tau S_2} & 1 & 0 & \cdots & \cdot & 0 \\ \dfrac{-b_{3,1}\tau S_1}{1+\tau S_3} & \dfrac{-b_{3,2}\tau S_2}{1+\tau S_3} & 1 & \cdots & \cdot & 0 \\ \cdot & \cdot & \cdot & \cdots & \cdot & \cdot \\ \cdot & \cdot & \cdot & \cdots & 1 & 0 \\ \dfrac{-b_{n,1}\tau S_1}{1+\tau S_n} & \cdot & \cdot & \cdots & & 1 \end{bmatrix}$

$$\hat{f} = \begin{bmatrix} \dfrac{1}{1+\tau S_1} & 0 & 0 & \cdots & 0 \\ 0 & \dfrac{1}{1+\tau S_2} & 0 & \cdots & 0 \\ 0 & 0 & \dfrac{1}{1+\tau S_3} & \cdots & 0 \\ \cdot & \cdot & \cdot & \cdots & \cdot \\ \cdot & \cdot & \cdot & \cdots & \cdot \\ \cdot & \cdot & \cdot & \cdots & \cdot \\ 0 & 0 & 0 & \cdots & \dfrac{1}{1+\tau S_n} \end{bmatrix}$$

Accordingly, from Eq. (4) and (11),

$$G = \hat{p}^{-1}\hat{f} \qquad (12)$$

In Eq. (9), specific breakage rate, S_i, and breakage distribution function, $b_{i,j}$, are obtained directly from experimental results but they can also be acquired by a few correlation equations indirectly. Herbst et al. [1968] gave a equation for S_i as follows:

$$S_i = S_1 \left[\frac{\overline{D}_i \overline{D}_{i-1}}{\overline{D}_1 \overline{D}_2} \right]^\alpha \qquad (i=1, 2, \cdots, n-1) \qquad (13)$$

where α is the constant.

For cumulative breakage distribution function, Austin et al. [1976] presented a correlation given by

$$B_{i,j} = \Phi_j \left[\frac{\overline{D}_i}{\overline{D}_j} \right]^\lambda + (1-\Phi_j) \left[\frac{\overline{D}_i}{\overline{D}_j} \right]^\theta \qquad (14)$$

$$(0 \le \Phi_j \le 1; \; j \le i \le n)$$

Accordingly, $b_{i,j}$ is defined as

$$b_{i,j} = B_{i-1,j} - B_{i,j} \qquad (j \le i \le n) \qquad (15)$$

From Eq. (13) and (14), we can see that S_i and $B_{i,j}$ are not affected by grinding time.
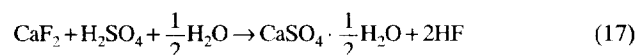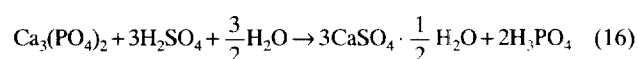
HEMIHYDRATE SECTION

Hemihydrate section, which consists of reaction stage and hemihydrate filtration stage, is the most important step in hemihydrate phosphoric acid process because the quality of product acid and that of crystal are determined in this section. So it is essentially required to keep the operating conditions of hemihydrate section within the optimal region.
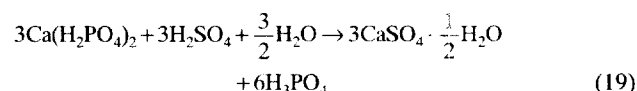
The purposes of reaction stage are to get pure and strong acid and to produce the hemihydrate crystal with good filterability. For these purposes, two principal operating parameters should be maintained within proper range. The first one is concentration of SO_4^{2-} ions in reaction liquid. In general hemihydrate crystals grow when the concentration of SO_4^{2-} is above the equilibrium level, but at high SO_4^{2-} concentration instant nucleations dominate and crystals cease to grow. Such small-sized nuclears can not be filtered easily. In addition, rock particles are coated by the nuclears and the coating hinders dissolution of rock. As a result, the recovery of P_2O_5 becomes poor and the efficiency of the process decreases. Therefore maintenance of the concentration of SO_4^{2-} within proper range is the most important.

The other parameter is the temperature of the reacting slurry. The higher the temperature, the stronger the coating effect, and the heat generated from reaction and dilution must be removed by a cooling system.

The main reaction in the hemihydrate process is for fluorapatite, $Ca_{10}(PO_4)_6F_2$, to react with sulfuric acid to produce phosphoric acid and hemihydrate crystal and is given by:

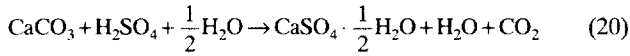$$Ca_3(PO_4)_2 + 3H_2SO_4 + \frac{3}{2}H_2O \rightarrow 3CaSO_4 \cdot \frac{1}{2}H_2O + 2H_3PO_4 \qquad (16)$$

$$CaF_2 + H_2SO_4 + \frac{1}{2}H_2O \rightarrow CaSO_4 \cdot \frac{1}{2}H_2O + 2HF \qquad (17)$$

Reaction (16) is completed through dissolution and crystallization which can be represented as

$$Ca_3(PO_4)_2 + 4H_3PO_4 \rightarrow 3Ca(H_2PO_4)_2 \qquad (18)$$

$$3Ca(H_2PO_4)_2 + 3H_2SO_4 + \frac{3}{2}H_2O \rightarrow 3CaSO_4 \cdot \frac{1}{2}H_2O + 6H_3PO_4 \qquad (19)$$

The above reactions can be described as a proton transfer mechanism [Becker, 1989]. The H^+ ions, which come from sulfuric acid and excessive phosphoric acid, attack phosphate rock particles to be dissolved into some materials including Ca^{2+} ions. Dissolved Ca^{2+} ions diffuse into the liquid solution and encounter SO_4^{2-} ions to form the hemihydrate crystals. Accordingly the overall reaction rate is controlled by the diffusion of reactants, especially of Ca^{2+} ions [Sluis et al., 1987]. Phosphate rock in-

cludes 10-15 components and each of these components causes side reactions. Among the side reactions, the principal reactive impurity is $CaCO_3$ which reacts as follows:

$$CaCO_3 + H_2SO_4 + \frac{1}{2}H_2O \rightarrow CaSO_4 \cdot \frac{1}{2}H_2O + H_2O + CO_2 \qquad (20)$$

In the reaction section many side reactions occur simultaneously and the mechanism of those reactions are so complex that it is very difficult to describe the reactions exactly. But some impurities amount to negligible quantity and many others are relatively unreactive, and reaction stage can be represented typically by the above reactions ignoring side reactions.

The type of crystals which are formed during reactions is determined by the time when nuclears are generated and depends on the temperature and phosphoric acid concentration. At high temperature and high P_2O_5 concentration, most crystals formed are hemihydrate. But, at some operating conditions, hemihydrate and dihydrate are in equilibrium, and conversion from one type to the other type takes place. Accordingly the reaction condition must be within the hemihydrate region, namely, above the hemihydrate-dihydrate transition point. Hemihydrate-dihydrate transition point can be represented by simple relations as

$$T_{tr,i} = 94.88 + 6.70C_{o,i} - 150.00C_{o,i}^2 \quad (where \ 0 \le C_{o,i} \le 0.3) \quad (21)$$

$$T_{tr,i} = 3.5 + 593.0C_{o,i} - 1100.0C_{o,i}^2 \quad (where \ 0.3 \le C_{o,i} \le 0.5) \quad (22)$$

The reaction stage being operated in Namhae Chemical Co. consists of 9 digesters and 2 vacuum coolers. For simplicity, it can be thought as being organized by 5 reactors and 1 vacuum cooler without the loss of its identity as shown in Fig. 3. Each reactor is assumed to be CSTR in which solid particles are suspended with acid. Return acid, which comes from hemihydrate filter, is introduced into R1, R2 and R3 so that phosphate rock should be sufficiently dissolved. In order for the dilution heat to be lessened and for the local supersaturation to be avoided sulfuric acid with concentration of 93 wt% is fed to R2 and R3 after it is mixed with return acid. Since most of reactions are exothermic and dilution of sulfuric acid generates large amount of heat, part of slurry from R4 is recycled to R3 through the vacuum cooler where high-temperature slurry is cooled by vaporization to keep the temperature of overall reaction section at 90-100°C. To increase the conversion of reaction and to guarantee the stability, part of slurry from R5 is recycled to R1. Most of the dissolution occurs in R1 and R2 and crystals grow mainly in R3, R4 and R5.

Steady-state mass balances on each reactor can be obtained by the incorporation of parameters which are given by

$$\delta = \left(\frac{f_c}{f_o}\right)\frac{M_o}{M_c}$$

$$\alpha_a = f_o \delta \frac{M_a}{M_o}$$

Phosphate rock, return acid and recycled slurry from R5 are introduced into R1. Slurry balance on R1 using the notation of Fig. 3 is given by

$$W_{s,1} = W_{pr,F} + \gamma W_{s,5} + W_{ra,1} \qquad (23)$$
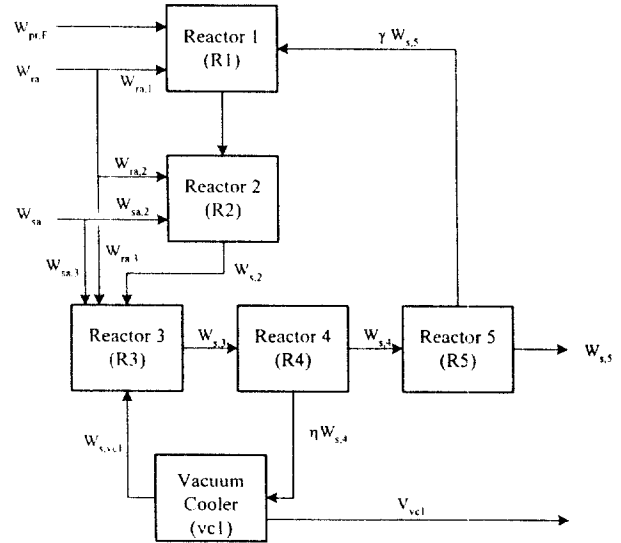

Fig. 3. Simplified structure of reaction stage.

The mass balance of undissolved rock and that of insoluble minors are given by

$$W_{pr,1} = (W_{pr,F} + \gamma W_{pr,5})(1 - \overline{X}_1) \qquad (24)$$

$$W_{im,1} = f_{im}\overline{X}_1(W_{pr,F} + \gamma W_{pr,5}) + \gamma W_{im,5} \qquad (25)$$

Liquid phase contains many components, and among them the amount of phosphoric acid, sulfuric acid and Ca^{2+} ion should be identified. The phosphoric acid balance can be written as

$$W_{sl,1}C_{p,1} = W_{ra,1}C_{p,ra} + \gamma W_{sl,5}C_{p,5}$$
$$+ 2f_o\overline{X}_1(W_{pr,F} + \gamma W_{pr,5})\frac{M_p}{M_o} \qquad (26)$$

and the sulfuric acid balance is given by

$$W_{sl,1}C_{a,1} = W_{ra,1}C_{a,ra} + \gamma W_{sl,5}C_{a,5} + f_a\overline{X}_1(W_{pr,F} + \gamma W_{pr,5})$$
$$- (W_{s,1}D_1 - \gamma W_{s,5}D_5)\frac{M_a}{M_h} \qquad (27)$$

The CaO balance can be written as

$$W_{sl,1}C_{c,1} = W_{ra,1}C_{c,ra} + \gamma W_{sl,5}C_{c,5} + f_c\overline{X}_1(W_{pr,F} + \gamma W_{pr,5})$$
$$- (W_{s,1}D_1 - \gamma W_{s,5}D_5)\frac{M_c}{M_h} \qquad (28)$$

Similarly balances at other reactors can be obtained. At reactor R3, slurry balance is given by

$$W_{s,3} = W_{s,2} + W_{sa,3} + W_{ra,3} + W_{s,vc1} \qquad (29)$$

and the balance of undissolved rock and that of insoluble minors are

$$W_{pr,3} = (W_{pr,2} + W_{pr,vc1})(1 - \overline{X}_3) \qquad (30)$$

$$W_{im,3} = f_{im}\overline{X}_3(W_{pr,2} + W_{pr,vc1}) + W_{im,2} + W_{im,vc1} \qquad (31)$$

The phosphoric acid balance and the sulfuric acid balance are represented respectively as

$$W_{sl,3}C_{p,3} = W_{ra,3}C_{p,ra} + W_{sl,2}C_{p,2} + W_{sl,vc1}C_{p,vc1}$$

$$+2f_o\overline{X}_3(W_{pr,2}+W_{pr,vc1})\frac{M_p}{M_o}\qquad(32)$$

$$W_{sl,3}C_{a,3}=0.93W_{sa,3}+W_{ra,3}C_{a,ra}+W_{sl,2}C_{a,2}+W_{sl,vc1}C_{a,vc1}$$
$$+f_a\overline{X}_3(W_{pr,2}+W_{pr,vc1})$$
$$-(W_{s,3}D_3-W_{s,2}D_2-W_{s,vc1}D_{vc1})\frac{M_a}{M_h}\qquad(33)$$

The CaO balance is given by

$$W_{sl,3}C_{c,3}=W_{ra,3}C_{c,ra}+W_{sl,2}C_{c,2}+W_{sl,vc1}C_{c,vc1}$$
$$-f_c\overline{X}_3(W_{pr,2}+W_{pr,vc1})$$
$$-(W_{s,3}D_3-W_{s,2}D_2-W_{s,vc1}D_{vc1})\frac{M_c}{M_h}\qquad(34)$$

At each reactor, solid particles are suspended in liquid phase and the slurry content of each phase is given by

$$W_{ss,i}=W_{pr,i}+W_{im,i}+W_{s,i}D_i\qquad(35)$$

$$W_{sl,i}=W_{s,i}-W_{ss,i}\qquad(36)$$

At vacuum cooler, water and a few kinds of volatile components are evaporated and the following relations can be written.

$$W_{s,vc1}=\eta W_{s,4}-\rho_{vc1}V_{vc1}$$
$$W_{pr,vc1}=\eta W_{pr,4},\ W_{im,vc1}=\eta W_{im,4},\ W_{s,vc1}D_{vc1}=\eta W_{s,4}D_4$$
$$W_{sl,vc1}C_{p,vc1}=\eta W_{sl,4}C_{p,4},\ W_{sl,vc1}C_{a,vc1}=\eta W_{sl,4}C_{a,4},$$
$$W_{sl,vc1}C_{c,vc1}=\eta W_{sl,4}C_{c,4}\qquad(37)$$

In the above equations, the value of decomposition ratio, $\overline{X}_i$, and hemihydrate content, D_i, can be obtained by the correlation equation which was presented by Yeo et al. [1991] and Giola et al. [1977] respectively.

At each reactor, a large amount of heat is generated and most of it originates from dilution of sulfuric acid and exothermic reactions including dissolution and crystallization. The effect of frictional heat generated by agitators is negligible compared with dilution and reaction heat. Most of the heat generated during the reaction is removed by vacuum cooler. Heat loss was assumed to be negligible in real plant [Becker, 1989].

With the above simplifications, heat balance at reactor R1 is given by

$$W_{pr,F}C_{ph,pr}(T_{pr,F}-T_0)+\gamma W_{pr,5}C_{ph,pr}(T_5-T_0)$$
$$+W_{ra,1}C_{ph,l}(C_{p,ra})(T_{ra}-T_0)+\gamma W_{sl,5}C_{ph,l}(C_{p,5})(T_5-T_0)$$
$$+\gamma W_{s,5}D_5C_{ph,h}(T_5-T_0)+\Delta H_{r,h}(W_{pr,F}+\gamma W_{pr,5})\overline{X}_1$$
$$=W_{pr,1}C_{ph,pr}(T_1-T_0)+W_{s,1}D_1C_{ph,h}(T_1-T_0)$$
$$+W_{sl,1}C_{ph,l}(C_{p,1})(T_1-T_0)\qquad(38)$$

Similarly, at reactor R3, the heat balance can be written as

$$W_{pr,2}C_{ph,pr}(T_2-T_0)+W_{pr,vc1}C_{ph,pr}(T_{vc1}-T_0)$$
$$+W_{sl,2}C_{ph,l}(C_{p,2})(T_2-T_0)+W_{ra,3}C_{ph,l}(C_{p,ra})(T_{ra}-T_0)$$
$$+W_{sl,vc1}C_{ph,l}(C_{p,vc1})(T_{vc1}-T_0)+W_{s,2}D_2C_{ph,h}(T_2-T_0)$$
$$+W_{s,vc1}D_{vc1}C_{ph,h}(T_{vc1}-T_0)+\Delta H_{r,h}(W_{pr,2}+W_{pr,vc1})\overline{X}_3$$
$$+W_{sa,3}[C_{ph,a}(T_{sa}-T_0)+0.93\Delta H_d]$$
$$=W_{pr,3}C_{ph,pr}(T_3-T_0)+W_{s,3}D_3C_{ph,h}(T_3-T_0)$$
$$+W_{sl,3}C_{ph,l}(C_{p,3})(T_3-T_0)\qquad(39)$$

At vacuum cooler the temperature of recycled slurry from R4 is lowered by vaporization and heat balance can be written as

$$\rho_{vc1}V_{vc1}\Delta H_v=\eta W_{sl,4}C_{ph,l}(C_{p,4})(T_4-T_0)$$
$$-W_{s,vc1}C_{ph,l}(C_{p,vc1})(T_{vc1}-T_0)$$
$$+\eta W_{pr,4}C_{ph,pr}(T_4-T_{vc1})$$
$$+\eta W_{s,4}D_4C_{ph,h}(T_4-T_{vc1})\qquad(40)$$

To compute the above equations we need to know specific heat of each component, heat of reaction, heat of dilution, etc. The values of average specific heat for solid components at 90-100°C and for 93% sulfuric acid are shown in Table 1. But for the liquid mixture of phosphoric acid, sulfuric acid and other soluble components average specific heat depends on concentration of each component. Because of the absence of experimental data, we have to rely on the actual operation data. Based on these data, the specific of heat of liquid solution is simply represented as

$$C_{ph,l}=0.980-0.796C_{p,i}\qquad(41)$$

Heat of reaction (16, 17) and dilution heat of sulfuric acid can be given by

$$-\Delta H_{r,h}=128.70-0.659T_i\qquad(42)$$

$$-\Delta H_d=211.044(C_{a,be}^2-C_{a,af}^2)\qquad(43)$$

Vaporization heat at vacuum cooler can be calculated by using Watson equation.

The slurry from reaction section is fed into the hemihydrate filter the type of which is belt-filter consisting of 3 sections as shown in Fig. 4. At the first section the filtrate is pumped to storage tank as product acid. Some part of the filtrate at first section is delivered to return acid tank. In second section, the filter cake is washed with third filtrate and second filtrate is consumed as return acid after adjusting P_2O_5 content by the first filtrate. After being dried in third section, hemihydrate cake is discharged and the cake is repulped with spray acid to be fed to the dihydrate section. During filtration it is assumed that no reactions take place.

The washing efficiency is defined as the ratio of soluble matter washed off in filter cake to total soluble matter before being washed. The washing efficiency is highly dependent on the size and the habit of hemihydrate crystal Therefore the conditions suitable for creation of crystal with good filterability should be maintained in reactors. The cake thickness has also significant effect on washing effect. Thin cake makes it possible to achieve higher washing efficiency, but sometimes cracking of cake may occur. Thus it is important to decide the proper cake thickness according to the size and crystal habit of hemihydrate.

From mass balances, the amount of liquid contained in cake

Table 1. Average specific heat of components

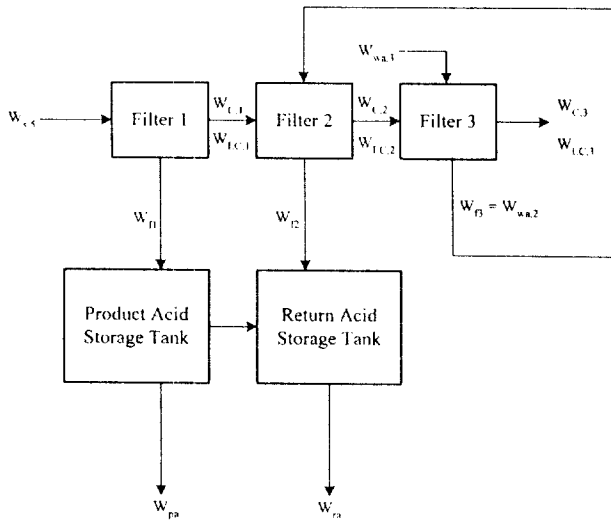| Component	Specific heat (kcal/kg-°C)
Phosphate rock $(C_{ph,pr})$	0.220
Hemihydrate crystal $(C_{ph,h})$	0.224
93% H_2SO_4 solution $(C_{ph,a})$	0.408

Fig. 4. Structure of hemihydrate filtration stage.

Fig. 5. Structure of hydration stage.

at each filtration stage can be calculated by

$$W_{LC,i} = W_{C,i}\left(\frac{X_{L,i}}{1-X_{L,i}}\right) \tag{44}$$

The filtrate at the first stage is separated into product acid and return acid, and mass balances on the first stage are given by

$$W_{f,1} + W_{LC,1} = W_{sl,5} \tag{45}$$

$$W_{f,1} = W_{f1,ra} + W_{pa} \tag{46}$$

The composition of product acid is the same as that of the liquid phase in slurry fed to the hemi-filtration section because no wash acid is introduced into the first filtration stage. At second filtration stage, the amount of filtrate can be computed by

$$W_{f,2} + W_{f1,ra} = W_{ra} \tag{47}$$

The balance of each component at return acid tank is given by

$$W_{f,2}C_{j,f2} + W_{f1,ra}C_{j,f1} = W_{ra}C_{j,ra} \quad (j=a, c, \text{ or } p) \tag{48}$$

At second filtration stage, the hemihydrate cake is washed by wash acid which comes from third filtrate and the balance can be written as

$$W_{wa,2} + W_{LC,1} = W_{LC,2} + W_{f,2} \tag{49}$$

The balance for each component on filter cloth is given by

$$(W_{f,2} - E_{wa,2}W_{LC,1})C_{j,wa2} + E_{wa,2}W_{LC,1}C_{j,f1} = W_{f,2}C_{j,f2} \tag{50}$$

$$W_{LC,2}C_{j,LC2} + W_{f,2}C_{j,f2} = W_{LC,1}C_{j,f1} + W_{wa,2}C_{j,wa2}$$
$$(j=a, c, \text{ or } p) \tag{51}$$

In the same way balances at third filtration stage can be obtained.

DIHYDRATE SECTION

Dihydrate section consists of hydration stage where hemihydrate cake is converted to dihydrate and dihydrate filtration
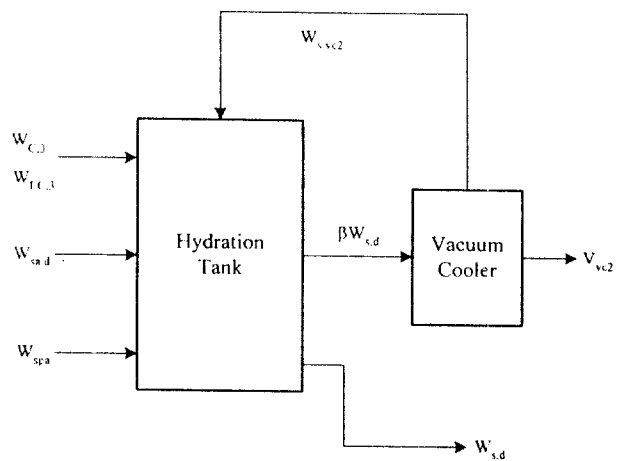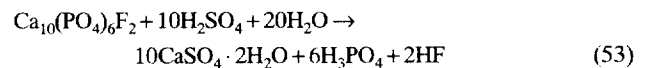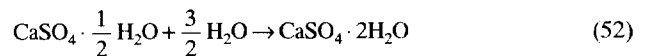
stage where gypsum is produced. Hemihydrate cake from hemihydrate filtration section is repulped with spray acid and then fed to the hydration stage. Sulfuric acid is also introduced into hydration tank and structure of the overall hydration section is shown in Fig. 5.

The principal phenomena in hydration stage are recrystallization and conversion of hemihydrate to dihydrate. As the temperature of slurry falls off below the hemihydrate-dihydrate transition point, the solubility of calcium sulfate in hemihydrate state decreases. This causes the wide solubility difference between hemihydrate and dihydrate and due to the difference of solubility the conversion of hemihydrate to dihydrate is accelerated. Through the hydration stage stable and big-sized crystal, which is filtered easily, is obtained due to the recrystallization. Moreover, undecomposed phosphate rock is dissolved almost completely in hydration tanks due to high sulfuric acid content, which results in high P_2O_5 recovery. The main reactions in hydration tank are

$$CaSO_4 \cdot \frac{1}{2}H_2O + \frac{3}{2}H_2O \rightarrow CaSO_4 \cdot 2H_2O \tag{52}$$

$$Ca_{10}(PO_4)_6F_2 + 10H_2SO_4 + 20H_2O \rightarrow$$
$$10CaSO_4 \cdot 2H_2O + 6H_3PO_4 + 2HF \tag{53}$$

The slurry balance at hydration tank is given by

$$(1+\beta)W_{s,d} = W_{LC,3} + W_{C,3} + W_{s,vc2} + W_{spa} + W_{sa,d} \tag{54}$$

and the balances for undecomposed rock and insoluble minors are given by

$$W_{pr,d} = (W_{pr,5} + W_{pr,vc2})\frac{(1-\overline{X}_d)}{(1+\beta)} = W_{pr,5}\frac{(1-\overline{X}_d)}{(1+\beta\overline{X}_d)} \tag{55}$$

$$W_{im,d} = W_{im,5} + f_{im}\overline{X}_d(W_{pr,5} + W_{pr,vc2}) \tag{56}$$

The phosphoric acid balance is written by

$$W_{sl,d}C_{p,d} = W_{LC,3}C_{p,C3} + W_{spa}C_{p,spa}$$
$$+ 2f_o\overline{X}_d(W_{pr,5} + W_{pr,vc2})\frac{M_{p-}}{M_o} \tag{57}$$
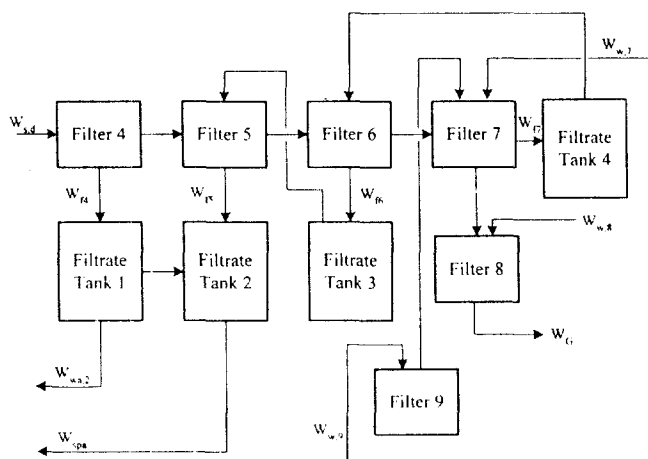
and the sulfuric acid balance is obtained as

Fig. 6. Structure of dihydrate filtration stage.

$$W_{sl,d}C_{a,d} + \alpha_a(W_{pr,5} + W_{pr,vc2})\overline{X}_d$$
$$= W_{LC,3}C_{a,C3} + 0.93W_{sa,d} + W_{spa}C_{a,spa}$$
$$+ f_a\overline{X}_d(W_{pr,5} + W_{pr,vc2}) \tag{58}$$

Both hydration and decomposition are exothermic reactions and 93% sulfuric acid causes a large amount of heat during dilution. The heat generated in hydration is removed by vacuum cooler and slurry temperature is maintained at about 60°C. The heat balance at the hydration tank can be obtained as

$$W_{LC,3}C_{ph,l}(C_{p,LC3})(T_{hf} - T_0) + W_{sl,vc2}C_{ph,l}(C_{p,vc2})(T_{vc2} - T_0)$$
$$+ W_{s,5}D_5C_{ph,h}(T_{hf} - T_0) + W_{s,vc2}D_{vc2}C_{ph,D}(T_{vc2} - T_0)$$
$$+ W_{pr,5}C_{ph,pr}(T_{hf} - T_0) + W_{pr,vc2}C_{ph,pr}(T_{vc2} - T_0)$$
$$+ W_{spa}C_{ph,l}(C_{p,spa})(T_{spa} - T_0) + W_{sa,d}[C_{ph,a}(T_{sa} - T_0)$$
$$+ 0.93\Delta H_d] + (W_{pr,5} + W_{pr,vc2})\overline{X}_d\Delta H_{r,d} + W_{s,5}D_5\Delta H_h\overline{X}_h$$
$$= (1 + \beta)[W_{sl,d}C_{ph,l}(C_{p,d}) + W_{s,d}D_dC_{ph,D}$$
$$+ W_{pr,d}C_{ph,pr}](T_d - T_0) \tag{59}$$

Heat of decomposition and hydration are given by

$$-\Delta H_{r,d} = 172.872 - 1.080T_d \tag{60}$$

$$-\Delta H_h = 26.768 + 0.065T_d \tag{61}$$

The average specific heat of dihydrate crystal, $C_{ph,D}$, is 0.269. The balances at vacuum cooler can be obtained in the same way as in hemihydrate section.

Dihydrate slurry from hydration tank is fed to dihydrate filter where gypsum is produced. The filtration section being operated in Namhae Chemical Co. is Bird-Prayon type filter with 30 pans. The filter can be simplified into 6 stages including 3 washing stages as shown in Fig. 6. By washing the cake repeatedly hydration filter produces pure gypsum which contains little soluble P_2O_5 and is suitable for production of cement retarder. The balances at dihydrate filter can be easily obtained in the same way as at the hemihydrate filter.

SIMULATION RESULTS AND DISCUSSIONS

The steady-state simulation was performed with the closed system which combines all the subsections.
1. Grinding Section

Table 2. The size distribution of unground rock

Mesh	n (size section)	D_i, mm	x (wt fraction)
+3.5	1	6.147	0.0030
+5	2	4.784	0.0056
+8	3	3.162	0.0136
+12	4	1.884	0.0125
+20	5	1.119	0.0305
+35	6	0.625	0.1244
+65	7	0.312	0.3847
+150	8	0.156	0.3592
+200	9	0.0089	0.0432
-200	10	0.064	0.0233

Table 3. The size distribution of ground rock

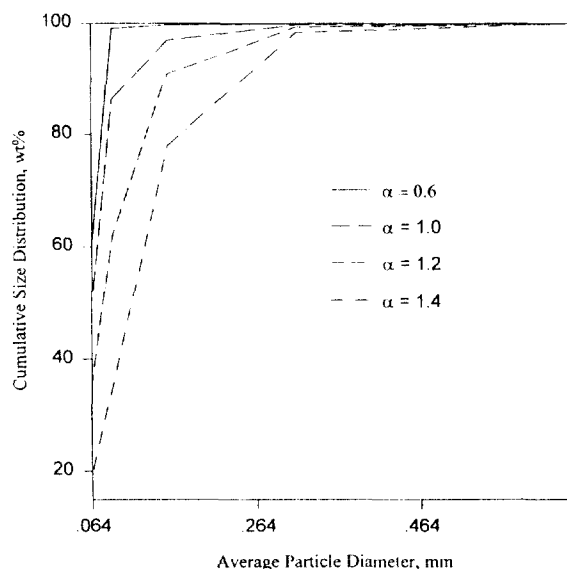| Mesh	Operation data	Simulation results
~+35	0.5% max	0.25%
-100~	75% min	97.1% (-150~)
-200~	50% min	50.5%

Fig. 7. The Effect of specific breakage rate on particle size distribution.

Table 2 shows the size distribution of unground rock fed to the ball mill unit. The size of feed rock is relatively small because the rock was ground once before being fed. According to operation data, the phosphate rock which is fed to the reaction stage after being ground by mill has the size distribution as shown in Table 3 and simulation results shows good agreement with the operation data.

In general the size distribution of ground rock particles is mainly affected by specific rate of breakage, S_i, which depends on the operating conditions and on the specifications of equipment such as the ball diameter, revolution speed of mill and the type of mill, etc. The effect of breakage rate on the particle size distribution was investigated by changing the constant α, and the simulation results are presented in Fig. 7. As α increases, i.e., the breakage rate at small size decreases, the breakage to small particles reduces remarkably. From this result it

Table 4. Standard operation conditions used in simulation

Feed rock (ton/hr)	150.4
composition (wt%):	
P_2O_5	31.3
CaO	46.0
SO_3	0.09
F	3.7
insol. min	11.4
Return acid (ton/hr)	
$W_{ra,1}$	204.7
$W_{ra,2}$	35.3
$W_{ra,3}$	48.7
compositions (wt%):	
P_2O_5	38.3
H_2SO_4	5.1
93% sulfuric acid (ton/hr)	
$W_{sa,2}$	46.4
$W_{sa,3}$	63.5
Recycle ratio	
η	1.7
ν	2.0
Temperature at vacuum cooler (°C)	60

Table 5. Simulation results for the standard operating conditions

Reactor no.	Operation data			Design value			Simulation results		
	T	P_2O_5	H_2SO_4	T	P_2O_5	H_2SO_4	T	P_2O_5	H_2SO_4
1	85-95	-	-	-	-	-	89.9	44.3	0.7
2	95-100	-	-	-	-	-	100.2	44.7	0.7
3	90-95	-	-	-	-	-	88.3	44.7	2.8
4	90-95	-	2-3	90	46.5	2.5	89.8	45.4	1.8
5	90-95	-	2-3	90	46.5	2.5	90.0	45.4	1.8
Vapor flow	-			391935.5			329193.7		

T	: reaction temperature (°C)
P_2O_5	: phosphoric acid concentration (wt%)
H_2SO_4	: sulfuric acid concentration (wt%)
Vapor flow	: the amount of vapor generated at vacuum cooler (m^3/hr)

can be seen that α should be below 1.0 to meet the size distribution shown in Table 3, and that α should be kept below the specific limit also in actual operation.

2. Hemihydrate Section

Table 4 shows standard operating conditions of hemihydrate section used in simulation and Table 5 shows simulation based on these conditions. Temperatures at each reactor are shown in Fig. 8. From the Fig. 8, we can see that the reactions take place in hemihydrate region, namely, at well above the hemihydrate-dihydrate transition point.

The simulation results agree well with the operation data and based on the reaction model the effect of principal manipulating parameters such as slurry recycle ratio could be examined. In reaction stage there are 2 recycle streams which are controlled by slurry recycle pumps. Fig. 9 shows the effect of inner recycle ratio, η, on the temperature at each reactor. From the figure, it can be found that the temperature at all reactors can be controlled by vacuum cooling system ant that η should be kept above 1.7 to maintain reaction temperature below 100°C.
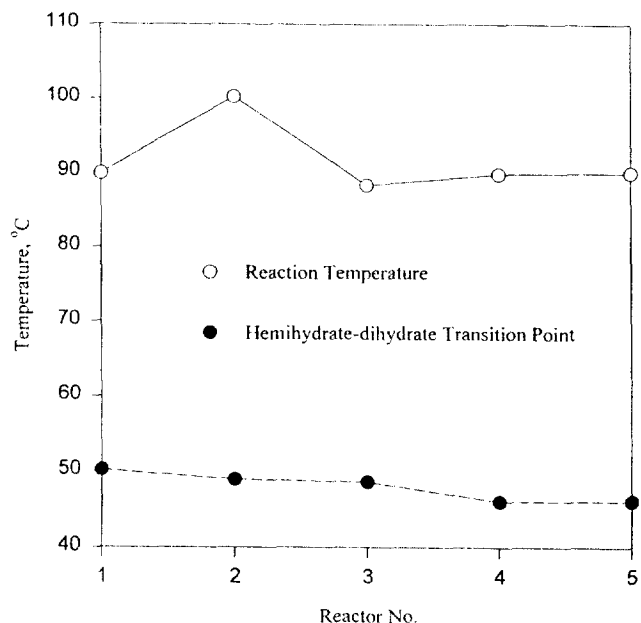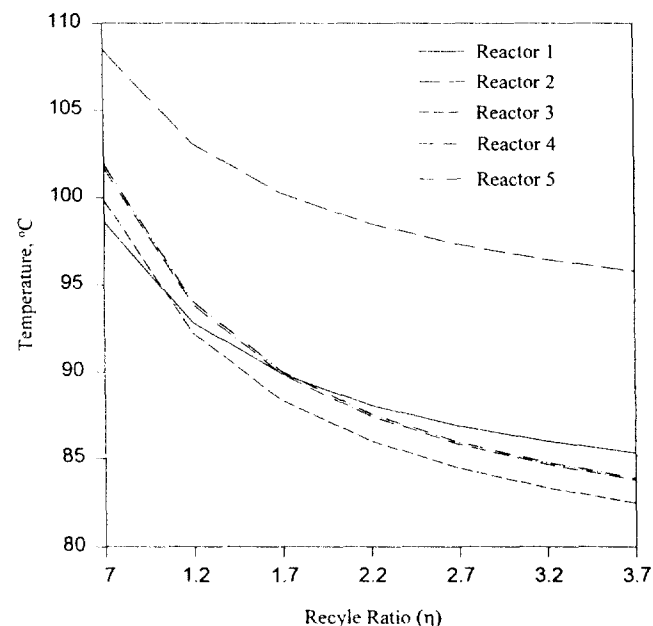

Fig. 8. Reaction temperature at each reactor.

Fig. 9. The effect of inner recycle ratio on the temperature at each reactor.

Fig. 10 shows that the P_2O_5 concentration at each reactor is little affected by η and is maintained approximately at 45%, which results in the production of rather strong acid. As can be seen in Fig. 11, the amount of vapor generated at vacuum cooler increases until $\eta<1.7$, and decreases when $\eta>1.7$. The reason is that the temperature of reactor 4 decreases so sharply that the difference of temperature between the slurry from reactor 4 and the slurry cooled at vacuum cooler reduces rapidly.

The other parameter which has effects on the reaction stage is outer recycle ratio, ν. Fig. 12 shows the temperature-reducing effect by increasing ν. From the figure we can see that the reaction temperature is controlled also by outer recycle ratio.
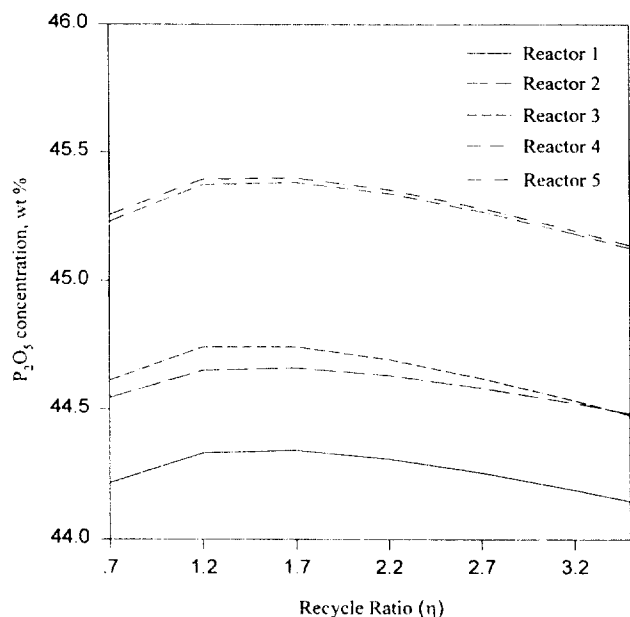
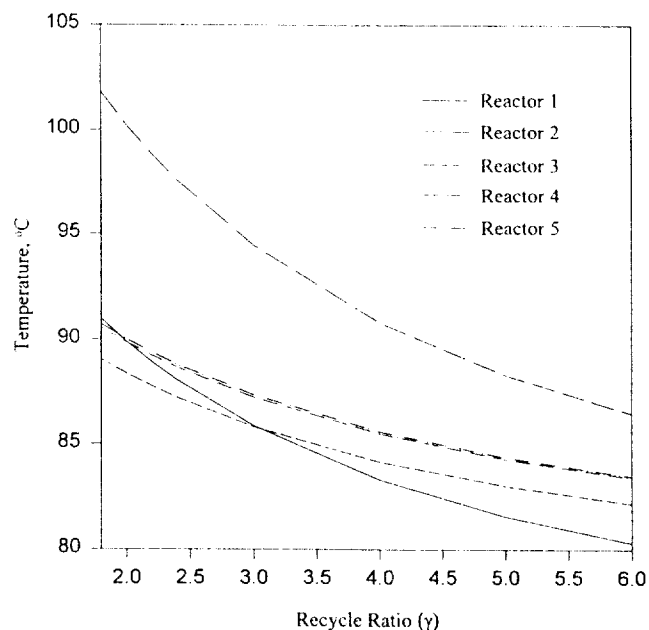**Fig. 10. The effect of inner recycle ratio on the phosphoric acid concentration.**

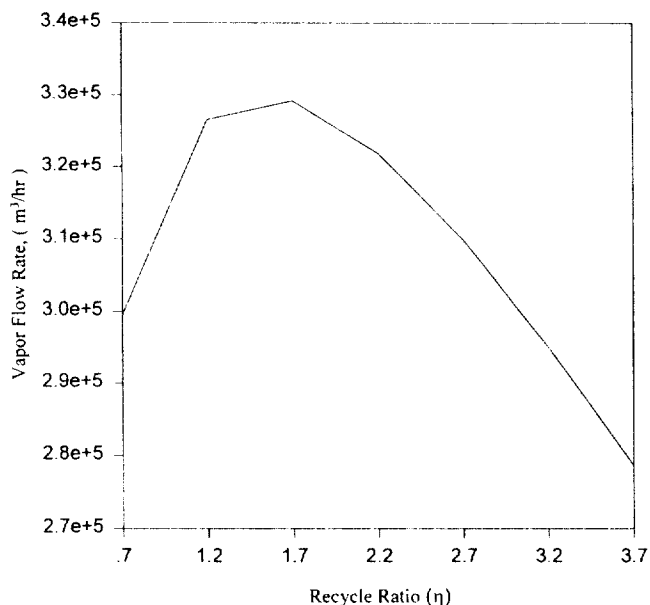**Fig. 12. The effect of outer recycle ratio on the temperature at each reactor.**

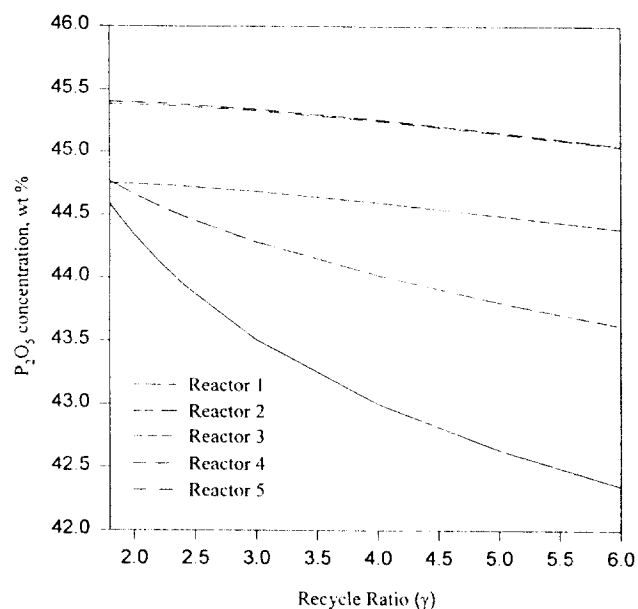**Fig. 11. The effect of inner recycle ratio on the amount of vapor generated.**

Fig. 13. The effect of outer recycle ratio on the phosphoric acid concentration.

The P_2O_5 concentration at some reactors is also affected but it is shown that the concentration at reactor 5 is maintained at relatively high level as shown in Fig. 13. The higher the recycle ratio, ν, the less the amount of vapor generated at vacuum cooler due to the decrease of slurry temperature as can be seen in Fig. 14.

3. Dihydrate Section

Table 6 shows the standard operating conditions of dihydrate section and Table 7 shows the simulation results. The simulation results show good agreement with the operation data. In hydration tank the reaction temperature must be kept below the hemihydrate-dihydrate transition point in order to ensure com-

pletion of the conversion of hemihydrate. The temperature is regulated by vacuum cooling system as in hemihydrate section. Fig. 15 shows the effect of recycle slurry on the temperature. It can be seen that the hydration takes place below the transition point and that the effect of recycle ratio on the temperature is negligible. On the other hand the amount of vapor which is generated at vacuum cooler depends on the recycle ratio as shown in Fig. 16.

CONCLUSION

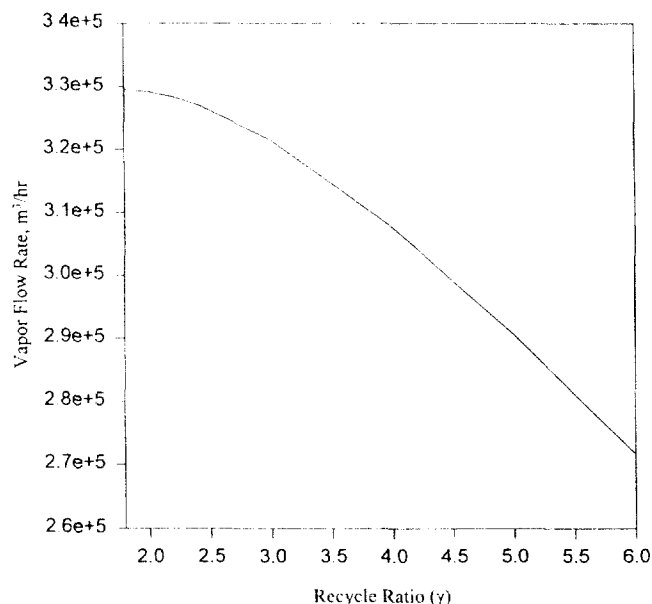A model for the actual wet hemihydrate phosphoric acid pro-

Fig. 14. The effect of outer recycle ratio on the amount of vapor generated.

Table 6. Standard operating conditions of dihydrate section

Sulfuric acid (93%)	18.2 (ton/hr)
Spray acid (8% P$_2$O$_5$)	312.5 (ton/hr)
Recycle ratio (β)	3.5
Temperature at vacuum cooler	55 (°C)

Table 7. Simulation results for the standard conditions

	Operation data	Design value	Simulation
Temperature (°C)	60	60	60.6
P$_2$O$_5$ (wt%)	10-15	11.1	11.6
H$_2$SO$_4$ (wt%)	5-10	6.0	8.0
Vapor flow generated (m^3/hr)	-	126000	112200

cess was developed to achieve optimal operation and design. The closed system consists of 3 subsections and simulation works were performed based on the model. From the results of simulations, the effects of some fundamental parameters at each unit were investigated. In grinding section it was found that the specific breakage rate has a great effect on the size distribution of ground rock particles and that it must be maximized for optimal operation. It was found to be possible to regulate the reaction temperature by using recycle ratios at reaction stage. Phosphoric acid could be produced at high concentration without being affected by the recycle ratios much. From the simulation results it was confirmed that stable transition of hemihydrate to dihydrate in hydration tank is possible.
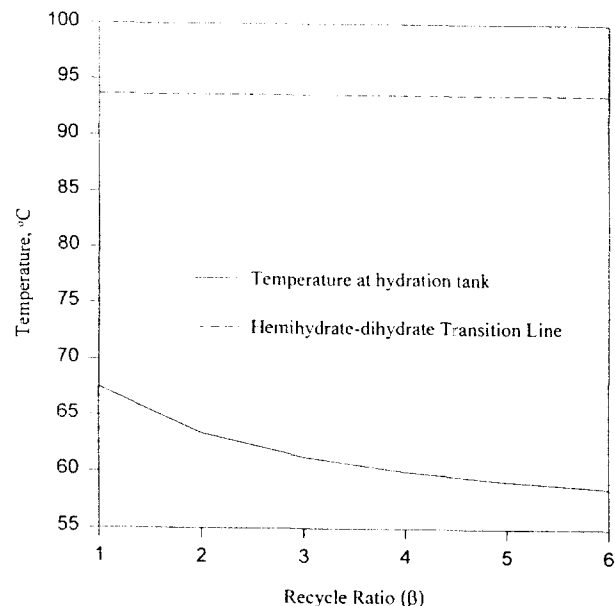
ACKNOWLEDGEMENT

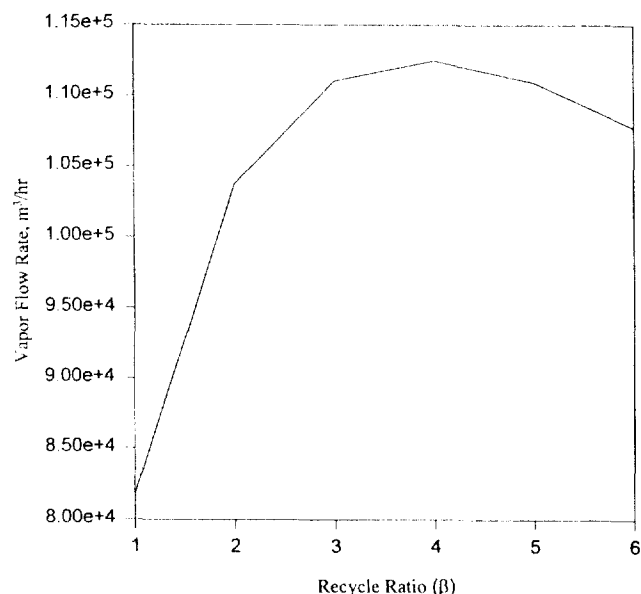Fig. 15. The effect of recycle ratio at hydration stage on the hydration temperature.

Fig. 16. The effect of recycle ratio at hydration stage on the amount of vapor generated.

NOMENCLATURE

B$_{ij}$: cumulative breakage distribution function
b$_{ij}$: breakage distribution function
C$_{i,j}$: concentration of component i in liquid solution from flow j [wt fraction]
C$_{ph,i}$: specific heat of matter i
D$_i$: hemihydrate or dihydrate content in the slurry flow i [kg crystal/kg slurry]
D̄$_i$: average diameter of particles belonging to size section i
E : separation efficiency matrix at grinding section
E$_{wa,i}$: washing efficiency at filter i

F : mixed feed vector to ball mill [kg/hr]

f$_i$: weight fraction of component i in phosphate rock

f$_i$: total mass flow rate of feed rock to ball mill in grinding section [kg/hr]

G : transfer matrix of ball mill

H : mass hold up of ball mill [kg]

M$_i$: molecular weight of component i

M$_F$, M$_P$, M : feed rate, product rate, mass flow rate at steady state respectively in grinding section [kg/hr]

P, P' : product vector from ball mill and separator respectively [kg/hr]

p$_i$: total mass flow rate of product at ball mill in grinding section [kg/hr]

R : unground feed rock vector in grinding section [kg/hr]

r$_i$: total mass flow rate of unground feed rock in grinding section [kg/hr]

S$_i$: specific breakage rate [hr^{-1}]

T$_i$: temperature at section i [°C]

T$_0$: standard temperature [°C]

T$_{tr,i}$: hemihydrate-dihydrate transition point at section i [°C]

V$_i$: vapor flow rate generated at vacuum cooler i [m^3/hr]

W$_{C,i}$, W$_{LC,i}$: mass flow rate of filter cake and liquid in cake respectively from filter i [kg/hr]

W$_{f,i}$: mass flow rate of filtrate at filter i [kg/hr]

W$_{f1,ra}$: mass flow rate from 1'st filtrate tank to return acid [kg/hr]

W$_{im,i}$, W$_{pr,i}$: mass flow rates of insoluble minors and phosphate rock respectively from section i [kg/hr]

W$_{pa}$, W$_{ra}$, W$_{spa}$: mass flow rate of product acid, return acid, and spray acid respectively [kg/hr]

W$_{ra,i}$: mass flow rate of return acid to section i [kg/hr]

W$_{sa,i}$: mass flow rate of sulfuric acid to section i [kg/hr]

W$_{s,i}$, W$_{sl,i}$, W$_{ss,i}$: mass flow rate of slurry, liquid solution in slurry, and solid in slurry respectively from section i [kg/hr]

x$_{F,i}$: weight fraction of feed rock in section i

$\overline{X}_h$: hydration ratio

$\overline{X}_i$: decomposition ratio of phosphate rock at section i

X$_{L,i}$: liquid content in cake [kg liquid/kg cake]

x$_{P,i}$: weight fraction of ground rock in section i

x$_{R,i}$: weight fraction of unground rock in section i

Greek Letters

α : breakage rate constant at grinding section

α$_a$: amount of anhydrous sulfuric acid per rock [kg H$_2$SO$_4$/kg rock]

β : recycle ration at hydration section

δ : mole ratio CaO/P$_2$O$_5$ in phosphate rock

ΔH$_d$: heat of dilution [kcal/kg H$_2$SO$_4$]

ΔH$_h$: heat of hydration [kcal/kg hemihydrate]

ΔH$_{r,h}$: heat of decomposition to hemihydrate [kcal/kg rock]

ΔH$_{r,d}$: heat of decomposition to dihydrate [kcal/kg rock]

ΔH$_v$: heat of vaporization [kcal/kg vapor]

ν : outer recycle ratio in hemihydrate section

η : inner recycle ratio in hemihydrate section

ρ$_i$: density of vapor at vacuum cooler i [kg/m^3]

θ, λ, Φ$_j$: constants at grinding section

Subscripts

a : H$_2$SO$_4$

af : after mixing

be : before mixing

c : CaO

C1, C2, C3 : cake at each filter

D : CaSO$_4$·2H$_2$O

d : hydration section

f1, f2 : filtrate flow at each filter

F : feed flow

h : CaSO$_4$·1/2H$_2$O

hf : hemihydrate filter

l : liquid phase

LC1, LC2, LC3 : liquid in cake at each filter

o : P$_2$O$_5$

p : H$_3$PO$_4$

pr : phosphate rock

ra : return acid flow

sa : sulfuric acid flow

spa : spray acid flow

vc1, vc2 : each vacuum cooler

wa2 : wash acid flow to second filter

REFERENCES

Austin, L., Shoji, K., Bhatia, V., Jindal, V. and Savage, K., "Some Results on the Description of Size Reduction as a Rate Process in Various Mills", Ind. Eng. Chem. Process Des. Dev., 15(1), 187 (1976).

Becker, P., "Phosphates and Phosphoric Acid", Marcell Dekker Inc., New York (1989).

Clayton, W. R. and Tanke, M. A., "Model and Applications of Heat and Material Balance Calculations in the Dihydrate Phosphoric Acid Process", 188th ACS Meeting (1984).

Giola, F., Mura, G. and Viola, A., "Analysis, Simulation, and Optimization of the Hemihydrate Process for the Production of Phosphoric Acid from Calcareous Phosphorites", Ind. Eng. Chem. Process Des. Dev., 16(3), 390 (1977).

Herbst, J. A. and Fuerstenau, D. W., "The Zero Order Production of Fine Sizes in Comminution and its Implications in Simulation", Trans. SME/AIME, 241, 538 (1968).

Rajamani, R. K. and Herbst, J. A., "Optimal Control of a Ball Mill Grinding Circuit-I. Grinding Circuit Modeling and Dynamic Simulation", Chem. Eng. Sci., 46(3), 861 (1991).

Sluis, S., Meszaros, Y., Marchee, W. G. J., Wesselingh, H. A. and Rosmalen, G. M., "The Disgestion of Phosphate Ore in Phosphoric Acid", Ind. Eng. Chem. Res., 26, 2501 (1987).

Yeo, Y. K., Cho, Y. S, Park, W. H. and Moon, B. K., "Simulation of the Dihydrate Process for the Production of Phosphoric Acid", KJChE, 8(1), 23 (1991).